Colloid Polym Sci 278:746–756 (2000)

ORIGINAL CONTRIBUTION

F. Huijs
J. Lang

Morphology and film formation of poly(butyl methacrylate)–polypyrrole core–shell latex particles

Received: 02 September 1999
Accepted: 21 December 1999

F. Huijs[1,2]
[1]TNO Institute of Industrial Technology
Eindhoven, The Netherlands

[2]University of Groningen
Department of Polymer Chemistry
Materials Science Center
Groningen, The Netherlands

J. Lang (✉)
Institut Charles Sadron
CNRS-ULP Strasbourg
6, rue Boussingault
67083 Strasbourg Cedex, France

Abstract Core–shell latex particles made of a poly(butyl methacrylate) (PBMA) core and a thin polypyrrole (PPy) shell were synthesized by two-stage polymerization. In the first stage, PBMA latex particles were synthesized in a semicontinuous process by free-radical polymerization. PBMA latex particles were labeled either with an energy donor or with an energy acceptor, in two different syntheses. These particles were used in a second stage as seeds for the synthesis of the core–shell particles. The PPy shell was polymerized around the PBMA core latex in an oxidative chemical in situ polymerization. Proofs for the success of the core–shell synthesis were obtained using nonradiative energy transfer (NRET) and atomic force microscopy (AFM). NRET gives access to the rate of polymer chain migration between adjacent particles in a film annealed at a temperature above the glass-transition temperature T_g of the particles. Slower chain migration of the PBMA polymer chains was obtained with the PBMA–PPy core–shell particles compared to rate of the PBMA polymer chain migration found with the pure, uncoated PBMA particles. This result is due to the coating of PBMA by PPy, which hinders the migration of the PBMA polymer chains between adjacent particles in the film. This observation has been confirmed by AFM measurements showing that the flattening of the latex film surface is much slower for the core–shell particles than for the pure PBMA particles. This result can again be explained by the presence of a rigid PPy shell around the PBMA core. Thus, these two complementary methods have given evidence that real core–shell particles were synthesized and that the shell seriously hinders film formation of the particles in spite of the fact that it is very thin (thickness close to 1 nm) compared to the size (750 and 780 nm in diameter) of the PBMA core. Transparency measurements confirm the results obtained by NRET and AFM. When the films are placed at a temperature higher than the T_g of PBMA, the increase in transparency is faster for films made with the uncoated PBMA particles than for films made with the coated PBMA particles. This result indicates again that the presence of the rigid PPy layer around the PBMA core reduces considerably the speed at which the structure of the film is modified when heated above the T_g of PBMA.

Key words Polypyrrole · Poly(butyl methacrylate) · Core-shell · Film formation · Transparency · Nonradiative energy transfer · AFM

Introduction

Core–shell latex particles are composite particles made of two different polymers, one polymer theoretically forms the core of the particles and the other polymer the shell of the particles. Core–shell latex particles have a great number of actual or potential applications. They also offer interesting models for fundamental work, for instance, the study of their internal structure by various methods including scattering or fluorescence methods or the study of their morphology through thermodynamic or physicochemical concepts involving, for instance, interfacial tension between the two polymers and between each polymer and the surrounding continuous phase of the dispersion. For instance, a rationalization of the morphology of composite particles has been suggested by Sundberg and coworkers [1, 2] in terms of interfacial energy between the polymer phases and between the polymers and the aqueous phases. The morphologies of composite latex particles, including core–shell structures, obtained from different types of polymerization, have been discussed along this line [2–5].

Core–shell particles are usually synthesized by emulsion polymerization consisting of at least two steps, which are supposed to favor the separation between the core–polymer and the shell–polymer; however, it is known that in practice core–shell particles are often difficult to obtain. This happens, for instance, when the compatibility, or the polymer glass–transition temperature, T_g, is favorable to partial mixing of the two polymers, or when there is no appreciable difference between the affinity of the two polymers for the water phase, or when the thickness of the shell is very thin compared to the size of the particle. Therefore, one of the first objectives is usually to control the morphology (external shape and internal composition) of the core–shell particles.

We were interested in the synthesis of composite particles made of a nonelectrical conductive core and an electrical conductive shell. The core is made of poly(butyl methacrylate) (PBMA) and the shell of polypyrrole (PPy). The final aim of this work is the formation of transparent, conductive films containing small quantities of PPy; therefore, the composite particle were made with a very small shell of PPy compared to the size of the PBMA core. In the present work we were mainly concerned with obtaining evidence for the existence of a real core–shell structure for our synthesized composite particles and with obtaining an insight into the influence of the thin shell on particle deformation and latex film formation. For this purpose three complementary methods were used: the nonradiative energy transfer (NRET) method, atomic force microscopy (AFM), and film transparency measurements. NRET allowed comparison of the PBMA chain migration between adjacent particles and AFM allowed comparison of the surface flattening for latex films made of pure PBMA particles, on the one hand, and of PBMA–PPy core–shell particles, on the other hand. Differences in the rate of chain migration and surface flattening should appear if real core–shell particles are synthesized. The transparency measurements give an indication of the disappearance of voids in the latex film. These voids can scatter light and therefore reduce the film transparency. The results obtained by these methods are presented in the following; however, it must be noted that in the past several other methods were employed for the study of core–shell particles, which we will recall first for the sake of comparison with the methods used here.

Transmission electron microscopy (TEM) methods were employed in the early 1970s to study the morphology of polystyrene (PS) latex particles synthesized by a two-stage seeded emulsion polymerization [6, 7]. A small quantity of butadiene was added to the styrene in the second stage of the polymerization. The core–shell structure of the particles was clearly visible by staining the butadiene with osmium. Other experiments made on the same PS latex particles, where tritiated styrene was used, confirmed this result [7]. TEM, in conjunction with the osmium tetroxide staining method, was used for the morphological characterization of PS particles embedded in a poly(isobutyl acrylate) (PIBA) phase [8]. Foamlike structures were observed where beats of PS were surrounded by a film or a shell of PIBA. The structure of poly(vinyl acetate)–poly(butyl acrylate) latex particles has been investigated by other authors [9, 10] using the staining method. It was shown that the batch-polymerized particles have a relatively large butyl acrylate rich core surrounded by a vinyl acetate rich shell, whereas particles synthesized by semicontinuous polymerization under starving conditions have a more homogeneous composition. These structures, determined by TEM, were in agreement with dynamic mechanical spectroscopy [9, 10], differential scanning calorimetry [10], and tensile strength [10] measurements made on the same systems. TEM was widely used to investigate the morphology of several types of composite latex particles, for instance, particles made of PBMA and PS using TEM alone [11] or in conjunction with other methods [12]. Core–shell [12] or anomalous structured [11] particles were found depending on the emulsion polymerization method used. PS–poly(methyl methacrylate) (PMMA) latex particles, synthesized with PS as seed particles, were found to have nonuniform morphologies [3], whereas PMMA–PS latex particles, synthesized with PMMA as seed particles, were found to have a core–shell structure [13]. The existence of particles with a core–shell structure was demonstrated by TEM for several other types of latexes, for instance, particles made of silicon oils–poly(glycidyl methacrylate)

[14], particles based on various combinations of vinyl acetate and acrylate monomers [15, 16], or particles made of polymers with different affinity for water, for instance, hydrophobic PS and amphiphilic poly(hydroxyethyl methacrylate) [17].

Other methods have been used for the study of the morphology of core–shell particles. Small-angle neutron scattering of PMMA–PMMA [15, 18], PMMA–PS [18], PS–PMMA [15], and poly(methyl methacrylate-*co*-styrene)–PMMA [18] composite particles, synthesized using deuterated monomers in the second stage of the polymerization, gave evidence for the existence of core–shell structures. High-resolution NMR was employed to characterize polybutadiene–PMMA core–shell particles [20, 21] and small-angle X-ray scattering was used to study, directly [22] or by a contrast variation method [23, 24], the internal structure of PS–PMMA latex particles. Evidence for a core–shell structure with a small interfacial region between PS (core) and PMMA (shell) were found with the contrast variation method [23, 24]. It was also shown that the internal structure of core–shell latex particles can be studied using light scattering [25]. Dynamic mechanical spectroscopy measurements [9, 10, 26] and AFM [27] gave arguments for the existence of structured core–shell particles. Titration methods can also be carried out for the study of latex particles bearing functional groups at the surface or in the shell of the particles [28, 29].

The study of the structure of core–shell latex particles with a conducting shell was limited for a long time to scanning electron microscopy (SEM) and electrical conductivity measurements [30]. SEM micrographs showed that no new particles were formed during the synthesis of PPy and, since the conductivity of the particles was as high as 0.25 S/cm, it was concluded that the PPy formed a shell around the seed latex particles. Later studies used, besides SEM and electrical conductivity, other techniques such as elemental microanalysis [31], TEM and electrophoretic mobility [32], IR spectroscopy and disk centrifuge photosedimentometry [33], X-ray photoelectron spectroscopy, time-of-flight secondary ion mass spectroscopy, Raman and UV–visible reflectance spectroscopy, and scanning force microscopy [34]. These studies showed that a thin and uniform layer of PPy is formed around the latex particles. It was also shown that another conducting polymer, polyaniline, forms a much less uniform layer [35] than PPy [33, 34] around the same polystyrene particles. Various other studies of the structure of the core–shell latex particles with a conducting shell were performed; however, the influence of the rigid conducting shell on film formation has not been studied so far. Wiersma et al. [32] measured the electrical conductivity of PPy/polyurethane coatings as a function of time at 120 °C, but they did not compare the film formation of coated and uncoated particles, nor did they mention any influence of the conducting shell on the film formation process.

Recently, fluorescence NRET was used by several authors [36–38] for the study of the internal structure of core–shell latex particles. Labeling of the core–polymer with the donor and the shell–polymer with the acceptor gave information on the extent of mixing between the core and the shell. The study of PMMA–PMMA core–shell particles synthesized by different emulsion polymerization methods showed great differences in the core–shell morphology depending on the type of polymerization [36]. On the other hand, great differences were found in the distribution of the core and shell polymers inside the composite particle depending on the nature of the acrylate polymer which was supposed to form the core and the shell of the particle [37, 38]. In the present study only the core of the particles was labeled with either the donor or the acceptor. Indeed, the shell of the present core–shell particles is very thin compared to the core and, therefore, the difference between the energy transfer associated with a perfect core–shell and with complete or partial mixing between the core and the shell was expected to be very small. Thus, it would have been difficult to decide, from the NRET measurements, if real core–shell particles were obtained or not. Besides, covalent and uniform incorporation of the probe along the PPy chain was not straightforward. Furthermore, PPy has a very high T_g; therefore, we do not expect that the PPy chains will migrate, but we expect that the PBMA chains from the core will penetrate through the PPy shell, thus giving the film mechanical strength. Instead, information on the success of the synthesis was obtained from the study of the energy transfer which results from the interparticle polymer (PBMA) chain migration occurring in a latex dry film brought to a temperature above the polymer (PBMA) T_g. This step of film formation is usually called autohesion or further gradual coalescence of the latex particle in the film. Comparison of the rate of polymer chain migration in a film made with PBMA and with PBMA–PPy particles did give an indication of the success of the synthesis. Moreover, comparison of the surface flattening of films made of PBMA particles and of PBMA–PPy core–shell particles gave complementary information on the success of the synthesis of the core–shell particles.

The aim of the NRET and AFM studies was not only to check if the coating of the PBMA particles by PPy was really achieved, it was also to determine the correlation which may exist between the interparticle chain migration or the surface film flattening and the development of the transparency of the films. Therefore, the development of the transparency of films annealed at different temperatures and for different periods of time was measured. The results are compared to the rate of film formation and surface flattening obtained from the NRET and AFM measurements.

Materials and methods

Materials

Butyl methacrylate (BMA) and potassium persulfate (KPS) were purchased from Aldrich. The donor, (9-phenanthryl)methyl methacrylate (PheMMA), and the acceptor, 9-anthryl methacrylate (AnMA), were synthesized following a recipe given elsewhere [39]. The hydroxyethylcellulose (HEC) stabilizer was kindly donated by Hercules. All other reagents (pyrrole, HCl, $FeCl_3$, H_2O_2) were purchased from Aldrich. The pyrrole monomer was distilled just before use. Water was freshly deionized and distilled before use.

Latex particle synthesis

The PBMA particles were synthesized by semicontinuous free-radical emulsion polymerization, without surfactant, using KPS as the initiator. Two polymerizations were undertaken: one for the synthesis of the particles labeled with the donor, PheMMA, and the other for the synthesis of the particles labeled with the acceptor, AnMA. In each case a pure PBMA seed was first prepared and the rest of the components, including the donor or the acceptor, were then slowly (starving conditions) added to the seed. Slow addition of the donor and the acceptor with the BMA monomer was necessary to ensure an uniform distribution of the donors and the acceptors inside the particles. About 1 mol% of donor and acceptor relative to BMA was used. The synthesis temperature was 80 °C and the duration of the polymerization was about 20 h. The PBMA latexes were dialyzed thoroughly in dialysis bags (Medicell International, MWCO 12-14000 Da) against demineralized water until the conductivity of the water outside the dialysis bag remained under 10 μS/cm. The PBMA latex particles were then used for the synthesis of the PBMA–PPy core–shell latex particles. A stoichiometric mixture of PBMA particles labeled with the donor and with the acceptor was first prepared. To this mixture, the nonionic stabilizer HEC was added in order to keep the latex stable during the synthesis of the conducting shell. Oxygen was removed by bubbling N_2 through the reaction mixture. The in situ polymerization of pyrrole was done at room temperature at a pH of about 1, using Fenton's (H_2O_2/Fe^{3+}) reagent, and the reaction was allowed to proceed overnight. Thus, the PBMA particles labeled with the donor and with the acceptor form the core of the PBMA–PPy core–shell latex particles. Moreover, an equal quantity of particles labeled with PheMMA and with AnMA is present in the dispersion containing the core–shell particles. The recipes for the synthesis of the PBMA particles (called latexes L1 and L2 when labeled with PheMMA and AnMA, respectively) and for the PBMA–PPy core–shell particles (called latex L3) are given in Table 1.

Latex particle size measurements

The particle size was determined on dry latex films by AFM. Films were prepared by casting 2–3 drops of dispersion onto freshly cleaved quartz plates and they were allowed to air-dry. The dry films were about 100 μm thick. The atomic force microscope used was a Nanoscope III from Digital Instruments (Santa Barbara, Calif.) working in the tapping mode with a tip oscillation frequency around 370 kHz. The piezoelectric translator could scan a maximum surface area of 12×12 μm^2 and worked in the height mode, which means that the force exerted on the film by the cantilever during scanning was kept constant. The spring constant of the cantilever was about 50 N m^{-1}. The diameter of the particles was obtained from the height profile (Fig. 1). The z-scale representation on the image in Fig. 1A is achieved using a gray color scale. The lighter the gray, the higher the corresponding value of z. Besides the determination of the size of the particles, AFM allowed the shape and the polydispersity in the size of the particles to be appreciated. Notice the hexagonal arrangements of the latex particles in Fig. 1A which results from their very low polydispersity in size. It was also checked, by taking AFM images in the course of the synthesis of the core–shell particles, that no formation of PPy particles occurred. This is a first result which indicates that PPy probably forms a shell around the PBMA particles. All particles investigated in this study have a spherical shape and a very low size polydispersity. The values of the particle diameter are given in Table 2 and represent an average of at least 30 measurements of the center-to-center distance between adjacent particles as shown in Fig. 1B.

Latex films for energy transfer and flattening measurements

Latex films used for the study of the further gradual coalescence and the study of the surface film flattening were prepared in the same manner as for the particle size measurements done by AFM. For the study of the PBMA latex particles in dry films, an equal number of particles labeled with the donor (particles L1) and with the acceptor (particles L2) was first prepared in dispersion. This dispersion was next used to prepare dry films for energy transfer and flattening measurements. In the case of the PBMA–PPy core–shell particles the dispersion contained an equal number of particles labeled with the donor and with the

Table 1 Recipe for the synthesis of the poly(butyl methacrylate) (*PBMA*) latex particles (latex L1 labeled with (9-phenanthryl)methyl methacrylate *PheMMA*, and latex L2 labeled with 9-anthryl methacrylate *AnMA*) and for the PBMA–polypyrrole (*PPy*) core–shell particles (latex L3)

Step	Composition	Latex L1	Latex L2	Step	Composition	Latex L3
Seed (batch) (80 °C)	Water (ml)	38.35	38.35	Seed	Dispersion of a stoichiometric mixture of latexes L1 and L2 (g)	25.63[a]
	Potassium persulfate (g)	0.068	0.068			
	Butyl methacrylate (ml)	2.01	2.01			
Slow step (80 °C) (20 h)	Water (ml)	111.53	103.86	Batch	Hydroxyethylcellulose (1 wt% aq. sol.) (g)	7.92
	Potassium persulfate (g)	0.072	1.22			
	Butyl methacrylate (ml)	35.39	37.74		Pyrrole (μl)	30
	PheMMA (g)	0.687	–		HCl (37% aq. sol) (μl)	400
	AnMA (g)	–	0.695		$FeCl_3$ (0.29 wt% aq. sol.) (μl)	121
					H_2O_2 (35%) (μl)	48

[a] The solid content of the dispersion is 12.1 wt%

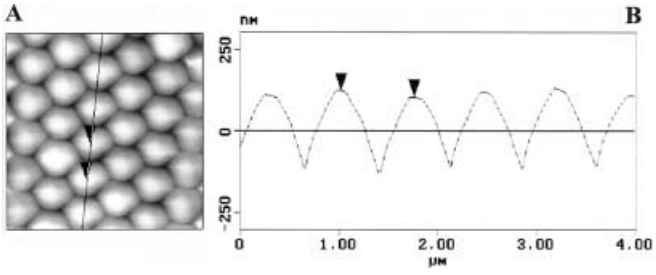

Fig. 1 Atomic force microscope top view (**A**) (size: 4 μm × 4 μm) and height profile (**B**) of L1 latex film. The height profile is taken along the *line* shown on the top view image. The diameter of the particles (750 nm) is obtained from the average distance between two adjacent *triangles*, which indicate the center of the particles, using the Nanoscope software

acceptor. Dry films were placed in an autoclave and heated for various periods of time at the desired annealing temperature (55, 70, 90, or 120 °C).

Fluorescence decay measurements

Donor (PheMMA) fluorescence decay traces were recorded with a single-photon counting apparatus [40]. Film samples, mounted on a homemade solid holder, were excited at 298 nm. The emission light was collected through a band-pass filter (Schott) centered at 366 nm to minimize the uptake of scattered and acceptor (AnMA) emitted light. All measurements were performed at 10 °C, i.e., below the T_g of the polymers, to avoid any kind of evolution of the particles in the films during the illumination time. The analysis of the decay profiles derives from the Förster equation of NRET [41]. It is based on the fact that the donors and the acceptors are static during the fluorescence measurements. The efficiency of the energy transfer is governed by the relation $E = R^6/(R^6+r^6)$, where R is the characteristic distance between the donor and the acceptor and is 23 Å for the couple phenanthrene–anthracene, which are the probes used in the present study, and r is the distance between a donor and an acceptor. Thus, the energy transfer depends only on the average donor–acceptor distance in the range 0–50 Å, which is small compared to the particle size (Table 2). This allows a precise determination of the extent of the PBMA chains migration between adjacent particles upon annealing the latex films at temperatures above the T_g (34 °C) of PBMA. The analysis of the donor fluorescence decay, $I(t)$, was first proposed by Zhao et al. [39], Pekcan et al. [42], and Wang et al. [43]. In this analysis the intensity, of the fluorescence emitted by the donor in the film is expressed by the sum of two contributions weighted by the preexponential factors B_1 and B_2, one of which comes from the domains where the donor is mixed with the acceptor and the other comes from the domains where the donor is without any acceptor in its vicinity:

$$I(t) = B_1 \exp[(-t/\tau) - p(t/\tau)^{1/2}] + B_2 \exp(-t/\tau) \quad . \tag{1}$$

In Eq. (1), p is a time-independent parameter proportional to the local concentration of acceptors and τ is the donor fluorescence lifetime that was found to be 46 ns in films containing only donor-labeled particles. The parameters B_1, B_2, and p are obtained by fitting Eq. (1) to the fluorescence decay data using a nonlinear weighted least-squares procedure. The apparent volume fraction of mixing, f'_m, between the polymer chains labeled with the donor and with the acceptor, has been defined from B_1 and B_2:

$$f'_m = B_1/(B_1 + B_2) \quad . \tag{2}$$

This fraction was corrected for energy transfer taking place through a perfectly neat interface between the donor- and the acceptor-labeled domains, $f'_m(i)$, and for energy transfer which occurs when the donor and acceptor domains are fully mixed, $f'_m(\infty)$, and was replaced by a normalized volume fraction of mixing, f_m, given by Eq. (3):

$$f_m = \left[f'_m - f'_m(i)\right] / \left[f'_m(\infty) - f'_m(i)\right] \quad . \tag{3}$$

The fraction of mixing $f'_m(\infty)$ was obtained from a film formed after dissolution in tetrahydrofuran (*THF*) of a stoichiometric mixture of dry particles L1 and L2 or from dissolution in THF of dry particles L3. Values of $f'_m(\infty)$ between 0.97 and 0.99, i.e., close to 1, which corresponds almost to complete mixing of PBMA chains labeled with PheMMA and AnMA, were found.

Flattening measurements

The topography of the film surface was determined by AFM, using the Nanoscope III working in the contact mode. The spring constant of the cantilever was 0.58 N m^{-1} and the piezoelectric translator again worked in the height mode. The flattening of the latex film surfaces was measured from the roughness, rms, obtained from the Nanoscope III software which corresponds to the quantity

$$\mathrm{rms}^2 = \frac{1}{N}\sum_{1}^{N}[z(i) - z_0]^2 \tag{4}$$

with

$$z_0 = \frac{1}{N}\sum_{1}^{N} z(i) \quad ,$$

where N is the number of z values used (512 × 512) and $z(i)$ is the height of point i. A surface area of 6 × 6 μm^2 was used for the measurement of the rms.

Table 2 Size of the latex particles synthesized determined by atomic force microscopy (*AFM*)

Latex	Composition	Probe	Diameter (nm)
L1	PBMA (homogeneous)	PheMMA	750 ± 20
L2	PBMA (homogeneous)	AnMA	780 ± 20
L3	PBMA–PPy (core–shell)[a]	Stoichiometric mixture of particles L1 and L2 labeled in the core with PheMMA and AnMA, respectively	770 ± 20

[a] The thickness of the shell is about 1 nm. This thickness is too small to be determined from the difference between the diameter of the PBMA–PPy and PBMA particles measured by AFM. From the recipe given in Table 1, the shell thickness is calculated to be 0.82 nm, taking 1.46 g cm^{-3} as the density of PPy

Transparency measurements

The transparency of the films was measured in situ using a home-built apparatus. Measurements were done on 2×2 cm^2 glass slides. The films were deposited on the glass slides by dip-coating the glass slides in the latex. The glass was corona-pretreated in order to improve the adhesion between the glass and the deposited film. The films were deposited and allowed to dry in an ambient atmosphere. The glass slide was then placed in a sample holder in an air-flow oven. The oven temperature was set to 25 °C for the first 2 min of the measurement and was then increased to the desired temperature (55, 70, 90, or 120 °C). The air temperature in the oven reached the set temperature in about 2 min. The temperature of the sample reached this temperature only after about 20 min due to the fact the heating of the metal components in the oven is rather slow. The transparency of the film was measured according to the following procedure. Two photodiodes (Siemens, BPW 21, wavelength 550 nm) were used; these were first calibrated using the same light source and an uncoated glass slide. One of the photodiodes, the reference, received the light directly from the light source, giving a signal S1. The other photodiode received the same light after it had passed through an uncoated glass slide, giving a signal S2. The calibration factor is given by the ratio S1/S2. The transparency of the film is determined using the same procedure, only the glass slide is coated with the latex film according to the procedure described earlier. The transparency of the film is given by the ratio S2/S1, corrected by the calibration factor.

Results and discussion

Nonradiative energy transfer

Figure 2 shows the variation of the fraction of mixing, f_m, versus the square root of the annealing time for the pure PBMA particles (Fig. 2A) and for the PBMA–PPy core–shell particles (Fig. 2B) annealed at four different temperatures, namely, 55, 70, 90, and 120 °C. Notice that in Fig. 2, as well as in the following figures, the square root of the annealing time has been used for the sake of clarity only. Some similar features appear for the two types of particles. One observes at each temperature an increase in f_m with the annealing time and, at a given annealing time, an increase in f_m with the annealing temperature. These are classical results which have already been observed by different authors [39, 43–50]. The increase in f_m with the annealing temperature has been attributed to the increase in the diffusion coefficient of the polymer chains as the temperature increases above the polymer T_g. Moreover, chain diffusion between adjacent particles takes time, and complete mixing can be obtained only after a certain time, which increases as the annealing temperature decreases. In Fig. 2, the longest annealing time is about 28 days which indicated that after 28 days, complete mixing between PheMMA and AnMA labeled polymer chains had not been achieved at 70 and 90 °C for both types of particles and that they would not be achieved for a very long time at 55 °C. Only at 120 °C is the mixing close to 1, around 0.9, after about 1 week.

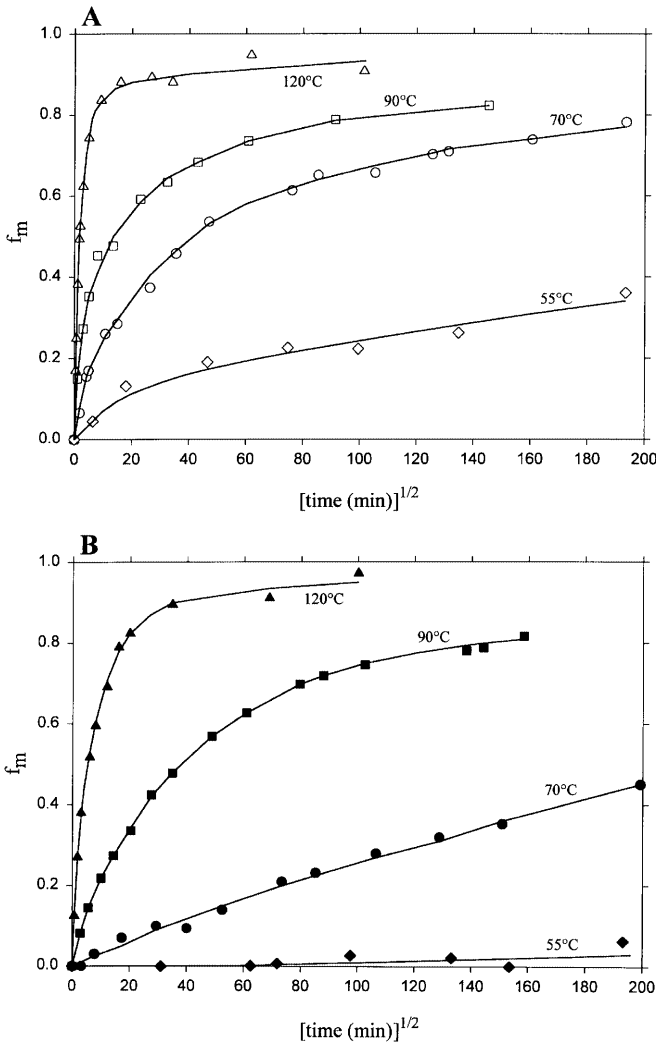

Fig. 2 Variation of the fraction of mixing, f_m, versus the annealing time for films made with **A** poly(butyl methacrylate) (*PBMA*) particles and **B** core–shell PBMA–polypyrrole (*PPy*) particles, annealed at 55 °C (✧, ◆), 70 °C (○, ●), 90 °C (□, ■), and 120 °C (△, ▲)

Although the behavior of the two types of particles appears roughly similar, large differences exist. Comparison of Fig. 2A and B shows that at a given annealing time, the fraction of mixing is, at each annealing temperature, larger in the case of the pure PBMA latex particles than in the case of the PBMA–PPy core–shell particles. This indicates that a modification of the PBMA particles happened when PPy was formed, which slows down the rate of migration of the PBMA polymer chains. This reduction in the rate of chain migration may have at least two origins. The first one is the presence of PPy particles between the PBMA particles, which reduces the contact between adjacent PBMA particles and, therefore, also reduces the interpenetration of PBMA polymer chains between adjacent particles and, thus, the fraction of mixing at a given

annealing time. However, this possibility can be discarded since the AFM images have not shown, as mentioned in the Materials and methods section, the presence of new particles of PPy after the second stage of the polymerization. Moreover, even if such particles had been present, they would have been present in very small quantities and would not have modified the fractions of mixing much. Indeed, the volume of PPy represents only about 1% of the volume of PBMA (Table 1). The second possible origin of the slowing down of the rate of PBMA chain migration is the formation of a PPy shell around the PBMA particles. Indeed, PPy is known to be a rigid polymer and, therefore, one can explain the slowing down of the rate of PBMA chain migration by assuming that PPy forms a barrier between the PBMA cores in the film, even if the shell thickness is very small. Recall that only the PBMA core is labeled and, therefore, only the mixing of the PBMA polymer chains is detected. Thus, in the case of the core–shell particle the detection of the mixing of the PBMA chain can be simply delayed by the presence of the PPy shell, even if the shell does not act as a barrier for the diffusion of PBMA and lets the PBMA diffuse through it without affecting the PBMA diffusion coefficient. Such delays have been evidenced in the study of other core–shell particles [51]. Here, however, the shell is too thin to give rise to delays as long as those shown in Fig. 2. The difference in the variation of f_m found between the coated and the uncoated particles is rather due to PPy acting as a real barrier for the diffusion of the PBMA chains through the interface which separates adjacent particles. This barrier probably has two origins. On the one hand, it results from the rigidity of PPy and, on the other hand, it arises from the thermodynamic incompatibility between PPy and PBMA. At the present time it is difficult to decide which of these two origins is the most likely.

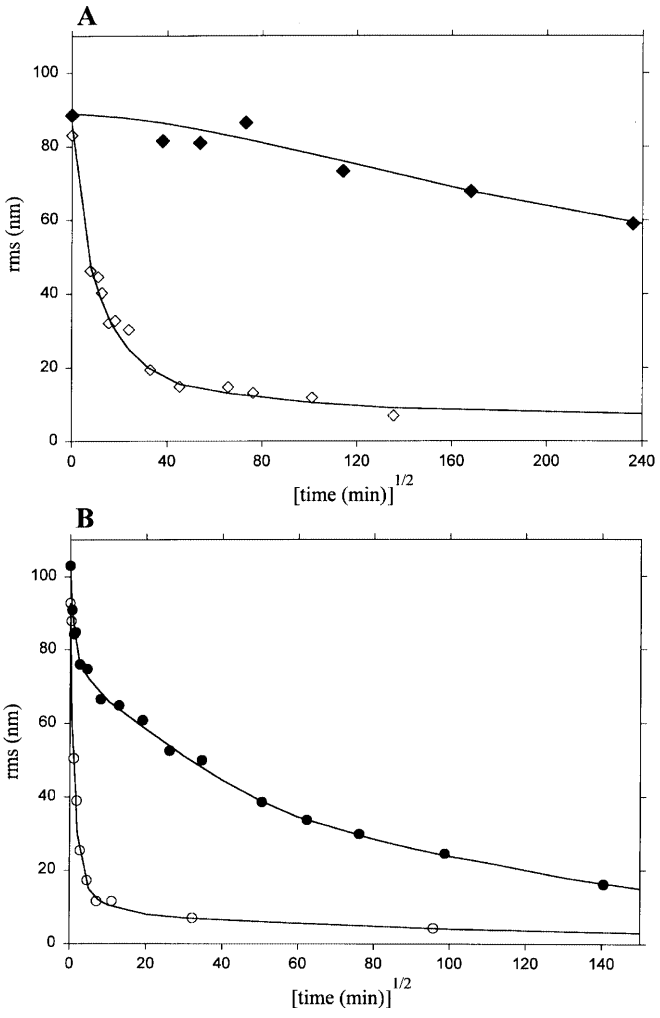

Fig. 3 Variation of the roughness (*rms*) versus the annealing time at **A** 55 °C and **B** 70 °C for films made with PBMA particles (✧, ○) and with core–shell PBMA–PPy particles (◆, ●)

Atomic force microscopy

The variation of the rms, determined by AFM for the PBMA–PPy core–shell and the pure PBMA particles is shown in Fig. 3. Figure 3A and B correspond to the flattening measured at 55 and 70 °C, respectively. One sees that as the annealing time increases the flattening measured for the pure PBMA film is faster than for PBMA–PPy films.

At 55 °C (Fig. 3A) the rms for the core–shell particles stays almost constant for a period of about 5 days. During the same period the rms of the pure PBMA particles decreases by a ratio close to 6 and almost reaches its minimum value. At 70 °C (Fig. 3B) there is also a large difference between the rms measured with the two types of particles. At a given annealing time, the rms, and therefore the roughness of the film surface, is larger for the film made with the PBMA–PPy core–shell particles than with the PBMA particles; however, at 70 °C the rms of the core–shell particles does not stay as constant as it does at 55 °C during the first 5 days. Due to its very small thickness, the shell of the particles can probably deform under the influence of the movement of the PBMA polymer chains, although its T_g is much higher than 70 °C. This deformation is larger at 70 °C than it is at 55 °C since the mobility of PBMA increases with temperature. This can explain the flattening of the PBMA–PPy latex film surface observed at 70 °C, which, however, stays much lower than the flattening observed at the same temperature with the uncoated PBMA particles. Thus, even in the case of the core–shell particles the viscoelastic relaxation of the latex particles seems to play a role in the film surface flattening. As done by other authors [52] in their studies of the flattening of latex film surfaces, we applied, as a part of

this work, the Williams–Landel–Ferry theory to our flattening data obtained with the pure PBMA and the core–shell PBMA–PPy latex particles. Figure 4 indicates that the time–temperature superposition principle indeed works for our uncoated and coated particles as well.

The results show that the study of the surface film flattening by AFM furnishes other evidence for the fact that a rigid shell is probably formed at the surface of the particles. Here again, if PPy particles had been synthesized during the second stage of the polymerization, i.e., if no coating of the PBMA particles with PPy had occurred, then such difference in surface film flattening between PBMA and PBMA–PPy particles would certainly not have been observed.

Comparison between interparticle chain migration and film flattening

An interesting result emerges from the comparison of the NRET and AFM data. This result does not concern the core–shell latex particles but it deserves to be mentioned since it answers partially the question of what the correlation between polymer chain migration between adjacent particles and surface film flattening is. In Fig. 5 we report the variations of the fraction of mixing and of the rms versus the annealing time at 55 °C (Fig. 5A) and 70 °C (Fig. 5B) for films made with the uncoated PBMA particles (mixture of an equal number of particles L1 and L2). This figure show that most of the film rms is considerably reduced when the fraction of mixing has attained a value close to 0.2–0.3 at both temperatures. A fraction of mixing of 0.3 corresponds to a penetration distance of the PBMA polymer chains between adjacent particles of only 13% of their diameter. It appears, therefore, that complete migration of the polymer chain between adjacent particles is not necessary for complete film flattening and that only a small part of the polymer chains was involved in the migration between adjacent particles when the complete flattening occurred. An identical result was previously obtained with PBMA latex particles of smaller size [53]. Comparison between the volumes involved in chain migration and in surface film flattening led to the conclusion that the rate of film flattening is faster than the rate based on simple polymer chain diffusion, because the polymer–air surface tension acts as an extra driving force in the flattening process [53]. Our result confirms the existence of this extra driving force. Note

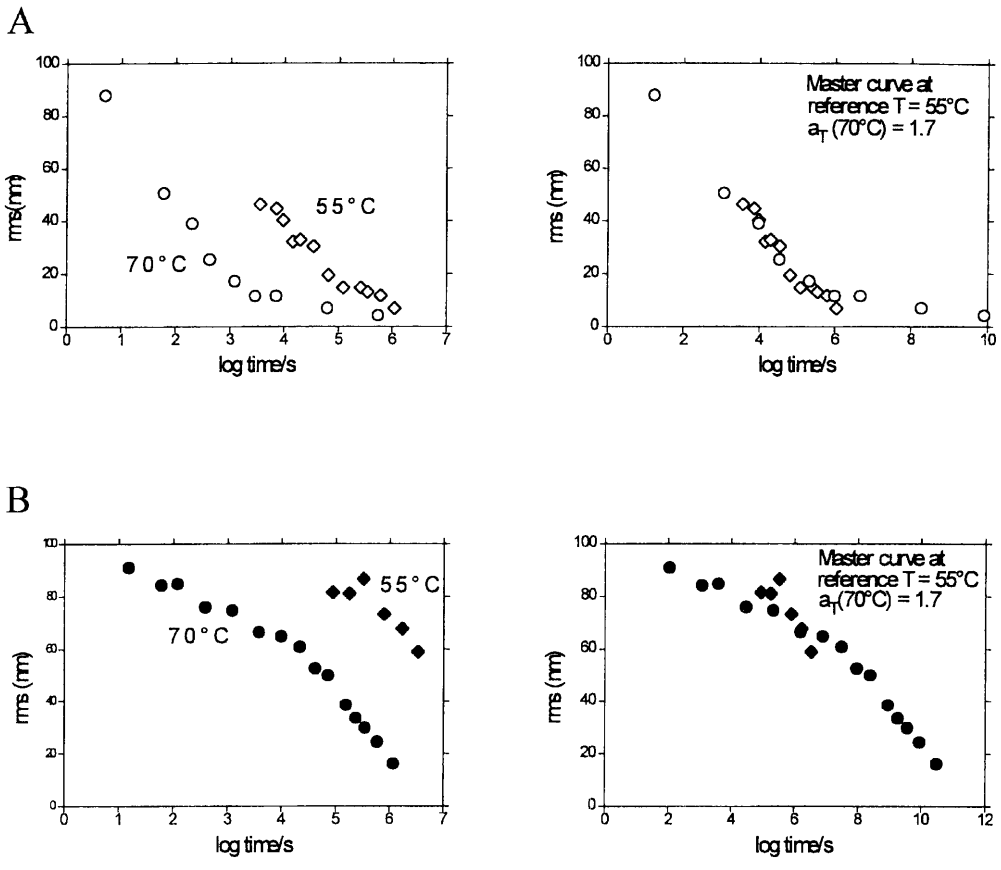

Fig. 4 Variation of the rms versus the logarithm of the time for **A** the uncoated and **B** the coated particles. The original data are shown in the *left figures*. Master curves obtained with the Williams–Landel–Ferry theory are shown in the *right figures*. The same shift factor, $a_T = 1.7$, was used to shift the data obtained with the uncoated and the coated particles

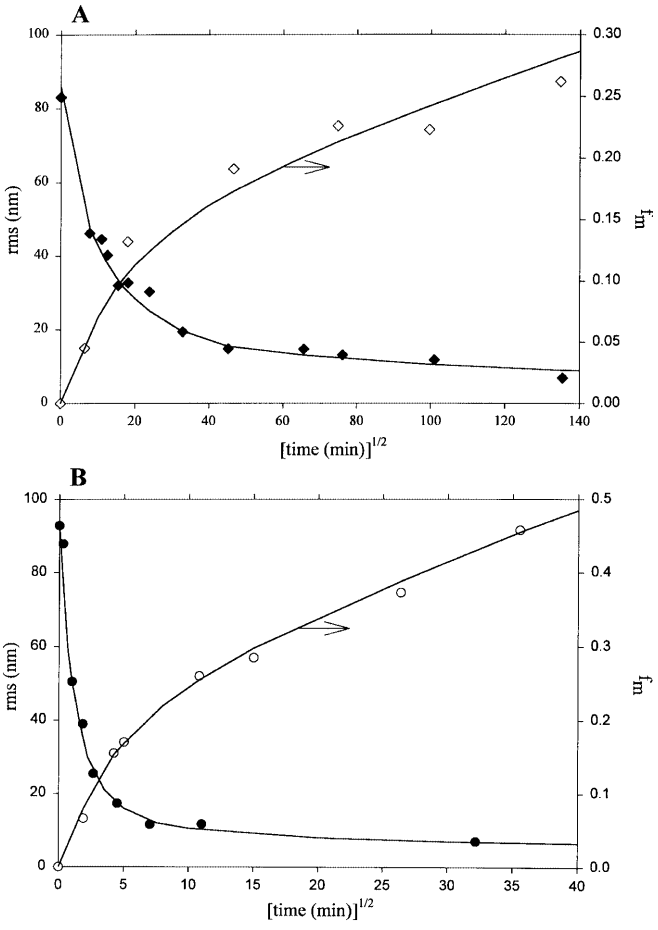

Fig. 5 Variation of the rms (◆, ●) and of f_m (✧, ○) versus the annealing time at **A** 55 °C and **B** 70 °C for films made with the PBMA particles

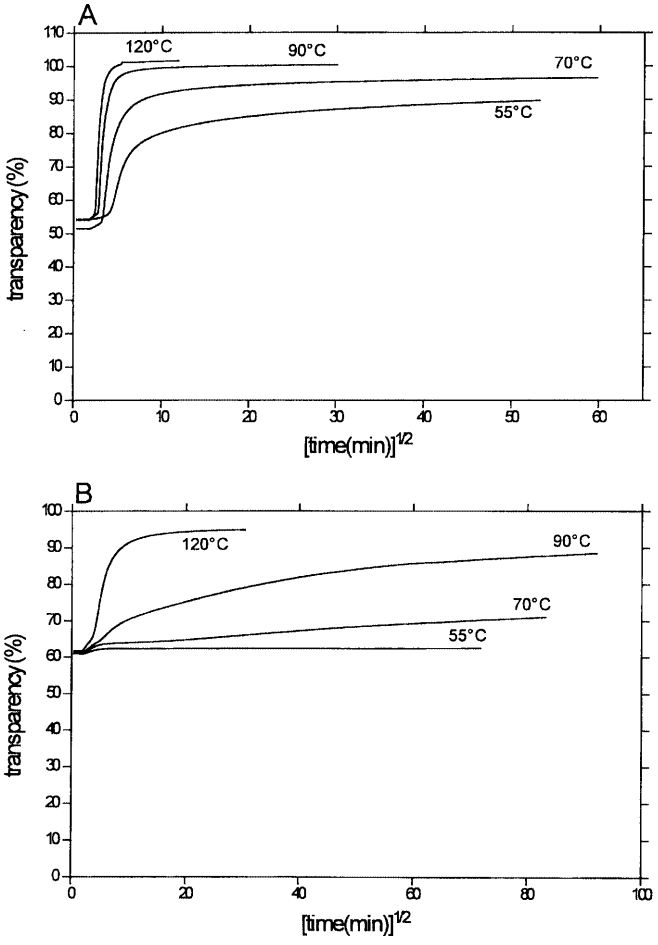

Fig. 6 Variation of the film transparency versus the annealing time at 55, 70, 90, and 120 °C for films made with **A** PBMA particles and **B** PBMA–PPy core–shell latex particles

that this result is in agreement with other results [54, 55] which indicate that the polymer chain diffusion constant, obtained from the corrugation height versus the annealing time, is larger than the diffusion constant of the polymer chain in the bulk, determined by NRET or small-angle neutron scattering.

Transparency measurements

Figure 6 shows the development of the transparency versus the square root of the annealing time for the pure PBMA particles (Fig. 6A) and for the PBMA–PPy core–shell particles (Fig. 6B), at 55, 70, 90, and 120 °C. At each temperature one observes an increase in the transparency of the films with time. Moreover, the rate of the transparency development increases as the temperature increases. Notice that at 55 °C the evolution of the film transparency is negligible for the film made with the coated particles, whereas a noticeable increase in the transparency is obtained for the film made with the uncoated particles. This result indicates that an appreciable difference occurs in the development of the transparency of the film made with the coated and the uncoated particles. At 70 °C, the transparency of the film made with the coated particle increases slightly and continuously, whereas for the film with the uncoated particles the transparency of the film increases very quickly and reaches more than 95% transparency in less than 2 h. At 90 and 120 °C, there is still a difference in the rate of transparency development between the films made with the coated and the uncoated particles, but this difference seems to decrease as the temperature increases.

A striking analogy appears between the NRET and the transparency results, if one compares the NRET results shown in Fig. 2 and the transparency results shown in Fig. 6. The rate of film formation and the rate of transparency development are slower for the films formed with the coated particles than for the films

formed with the uncoated particles. Moreover, close comparison between the NRET and the transparency results for each temperature indicates that film formation and transparency progress is parallel. For instance, in the case of the films made with the coated particles, the fraction of mixing stays almost constant at 55 °C, as does the transparency. At 120 °C, the transparency of the film made with the uncoated particles attains its plateau value (100% transparency) in about 15 min. After the same period of time the fraction of mixing is 0.7. With the film formed from the coated particles the transparency attains its plateau value (95% transparency) after a longer period of time, around 2 h, which is the time needed to obtain, for the same film, a value of f_m of 0.7. These results again show the correlation existing between the evolution of the fraction of mixing and the transparency of the films. This correlation is due to the fact that both the energy transfer and the disappearance of the voids increase with the diffusion of the PBMA polymer chains in the film.

A correlation also exists between film flattening and transparency development. This correlation appears when one compares the AFM results given in Fig. 3 and the transparency developments shown in Fig. 6 at 55 and 70 °C. At 55 °C, during a period of about 4 days, the roughness of the film surface as well as the film transparency stay almost constant for the films made with the coated particles, whereas a great decrease in the film roughness, which attains its minimum value, and a large increase in the transparency, which attains its maximum value, occur during the same period of time for films made with the uncoated particles. The same type of correlation can be made between film flattening and film transparency at 70 °C.

Thus, besides the correlation which exists between the evolution of the fraction of mixing and the transparency, there is also a correlation between the evolution of the roughness of the film and the transparency. It is known that voids existing in films formed at a temperature below the T_g of the particles diffuse the light and decrease the film transparency [56]. This is the case here for our nascent films. By annealing the films above the PBMA T_g, the particles can deform and the PBMA polymer chains can migrate between adjacent particles. The reduction in the size and in the number of the voids during film formation gives rise to an increase in the transparency of the films. Notice that complete mixing of the polymer chains belonging to adjacent particles is not necessary for the disappearance of the voids. The disappearance of the voids may occur much earlier than the complete mixing of the polymer chain in the film. We have, indeed, observed that the film transparency attains a plateau value, as the fraction of mixing is still around 0.7. Another factor that affects the film transparency is the reflection of the light at the surface of the film. We have shown that a correlation also exists between film flattening and film transparency; therefore, the effect of light reflection on the film transparency cannot be neglected. However, more work must be done, for instance, measurements of the refection of the light as a function of the roughness of the film, to obtain a definitive answer concerning the respective role played by the voids and by the film roughness on the film transparency.

Conclusion

PBMA–PPy core–shell particles with a very thin shell (thickness 1 nm) compared to the core (750 and 780 nm in diameter) were synthesized by two-step polymerization. Since core–shell particles are not always easy to synthesize, it was found necessary to control the structure before performing other experiments with them. Their structure was controlled using NRET and AFM. The results show that

1. No new nucleation occurred in the second stage during which polymerization of PPy was performed (AFM).
2. The migration of the PBMA polymer chain between adjacent particles in the films is slower with the PBMA–PPy core–shell particles than with the PBMA particles (NRET), indicating the presence of a barrier to the diffusion of the PBMA polymer chain in the first case.
3. The flattening of the surface of the latex dry film is faster with the PBMA particles than with the PBMA–PPy core–shell particles (AFM), indicating the presence of a rigid cap around the PBMA core in the second case.

These three results converge to the same conclusion, which is that it is very likely that PBMA–PPy core–shell particles were effectively synthesized. It was shown that the rate of the development of the transparency of the film increases with time when the films are at temperatures above the T_g of PBMA (T_g = 34 °C), increases with the temperature for a given annealing time, and is faster for the films formed with the PBMA particles than for the films made with the PBMA–PPy core–shell particles. This last result confirms the formation of a PPy shell around the PBMA particles. Film formation is accompanied by a deformation of the particles, a diffusion of the PBMA chains between adjacent particles, and a diminution of the size and of the number of the voids which scatter light inside the film. The diminution of the size and of the number of the voids is partly the origin of the increase in transparency during film formation. Another origin of the increase in film transparency upon film annealing is supported by the correlation existing between the flattening of the films and the development of their

transparency. As the flattening of the film increases, the reflection of the light at the surface of the film probably decreases and this may contribute to the increase in the film transparency. More work must be done in order to determine the part played by the decrease in the rms of the film surface on the transparency of the film upon film annealing.

Acknowledgements The authors wish to thank Frank Vercauteren (TNO), Barteld de Ruiter (TNO), Paul van Hutten (University of Groningen, Department of Polymer Chemistry), and Georges Hadziioannou (University of Groningen, Department of Polymer Chemistry) for valuable discussion. F.H. appreciates the financial support provided by the Senter IOP Surface Technology (IOT 95001 B), especially the extra financial support for a stage at the ICS.

References

1. Sundberg DC, Casassa AP, Pantazopoulos J, Muscato MR, Kronberg B, Berg J (1990) J Appl Polym Sci 41:1425
2. Sundberg EJ, Sundberg DC (1993) J Appl Polym Sci 47:1277
3. (a) Chen YC, Dimonie V, El-Aasser MS (1991) Macromolecules 24:3779; (b) Chen YC, Dimonie VL, Shaffer OL, El-Aasser MS (1993) Polym Int 30:185
4. (a) Lee S, Rudin A (1992) J Polym Sci Part A Polym Chem 30:865; (b) Lee S, Rudin A (1992) J Poly Sci Part A Polym Chem 30:2211
5. (a) Chen YC, Dimonie V, El-Aasser MS (1991) J Appl Polym Sci 42:1049; (b) Chen YC, Dimonie V, El-Aasser MS (1992) J Appl Polym Sci 45:487
6. Grancio MR, Williams DJ (1970) J Polym Sci A1 8:2617
7. Keusch P, Williams DJ (1973) J Polym Sci Polym Chem Ed 11:143
8. Kanig G, Neff H (1975) Colloid Polym Sci 253:29
9. Misra SC, Pichot C, El-Aasser MS, Vanderhoff JW (1979) J Polym Sci Polym Lett Ed 17:567
10. Misra SC, Pichot C, El-Aasser MS, Vanderhoff JW (1983) J Polym Sci Polym Chem Ed 21:2383
11. Okubo M, Katsuta Y, Matsumoto T (1982) J Polym Sci Polym Lett Ed 20:45
12. Min TI, Klein A, El-Aasser MS, Vanderhoff JW (1983) J Polym Sci Polym Chem Ed 21:2845
13. Jönsson JE, Hassander H, Törnell B (1994) Macromolecules 27:1932
14. He W, Tong J, Wang M, Pan C, Zhu Q (1995) J Appl Polym Sci 55:667
15. Hergeth WD, Bittrich HJ, Eichhorn F, Schlenker S, Schmutzler K, Steinau UJ (1989) Polymer 30:1913
16. Vandezande GA, Rudin A (1994) J Coat Technol 66:99
17. Kamei S, Okubo M, Matsumoto T (1986) J Polym Sci Polym Chem Ed 24:3109
18. (a) O'Reilly JM, Melpolder SM, Fisher LW, Wignall GD, Ramakrishnan V (1983) Polym Prepr Am Chem Soc Div Polym Chem 24:407; (b) Fischer LW, Melpolder SM, O'Reilly JM, Ramakrishnan V, Wignall GD (1988) J Colloid Interface Sci 123:24
19. Wai MP, Gelman RA, Fatica MG, Hoerl RH, Wignall GD (1987) Polymer 28:918
20. Tembou Nzudie D, Delmotte L, Riess G (1991) Makromol Chem Rapid Commun 12:251
21. Tembou Nzudie D, Delmotte L, Riess G (1994) Macromol Chem Phys 195:2723
22. Grunder R, Urban G, Ballauff M (1993) Colloid Polym Sci 271:563
23. Dingenouts N, Ballauff M (1993) Acta Polym 44:178
24. Ballauff M (1994) Macromol Symp 87:93
25. Manzur A (1994) J Colloid Interface Sci 162:197
26. Cavaillé JY, Jourdan C, Kong XZ, Perez J, Pichot C, Guillot J (1986) Polymer 27:693
27. Sommer F, Tran Minh Duc, Pirri R, Meunier G, Quet C (1995) Langmuir 11:440
28. Dobler F, Pith T, Holl Y, Lambla M (1992) J Appl Polym Sci 44:1075
29. Muroi S, Hashimoto H, Hosoi K (1984) J Polym Sci Polym Chem Ed 22:1365
30. Yassar A, Roncali J, Garnier F (1987) Polym Commun 28:103
31. Lascelles SF, Armes SP (1995) Adv Mater 7:864
32. Wiersma AE, van der Steeg LMA, Jongeling TJM (1995) Synth Met 71:2269
33. Lascelles SF, Armes SP (1997) J Mater Chem 7:1339
34. Lascelles SF, Armes SP, Zhdan PA, Greaves SJ, Brown AM, Watts JF, Leadly SR, Luk SY (1997) J Mater Chem 7:1349
35. Barthet C, Armes SP, Lascelles SF, Luk SY, Stanley HME (1998) Langmuir 14:2032
36. Winnik MA, Xu H, Satguru R (1993) Makromol Chem Macromol Symp 70/71:107
37. Pérez E, Lang J (1996) Langmuir 12:3180
38. Pérez E, Lang J (1999) J Phys Chem B 103:2072
39. Zhao CL, Wang Y, Hruska Z, Winnik MA (1990) Macromolecules 23:4082
40. Pfeffer G, Lami H, Laustriat G, Coche A (1963) C R Hebd Seances Acad Sci 257:434
41. (a) Förster Th (1948) Ann Phys (Leipzig) 2:55; (b) Förster Th (1959) Discuss Faraday Soc 27:7
42. Pekcan Ö, Winnik MA, Croucher MD (1990) Macromolecules 23:2673
43. Wang Y, Zhao CL, Winnik MA (1991) J Chem Phys 95:2143
44. Wang Y, Winnik MA (1990) Macromolecules 23:4731
45. Wang Y, Winnik MA, Haley F (1992) J Coat Technol 64:51
46. Wang Y, Winnik MA (1993) Macromolecules 26:3147
47. Wang Y, Winnik MA (1993) J Phys Chem 97: 2507
48. Boczar EM, Dionne BC, Fu Z, Kirk AB, Lesko PM, Koller AD (1993) Macromolecules 26:5772
49. Juhué D, Lang J (1994) Macromolecules 27:695
50. Juhué D, Lang J (1995) Macromolecules 28:1306
51. Marion P, Beinert G, Juhué D, Lang J (1997) J Appl Polym Sci 64:2409
52. Lin F, Meier DJ (1996) Langmuir 12:2774
53. (a) Pérez E, Lang J (2000) Langmuir 16:1874; (b) Pérez E, Lang J (1999) Macromolecules 32:1626
54. Goh MC, Juhué D, Leung OM, Wang Y, Winnik MA (1993) Langmuir 9:1319
55. Park YJ, Khew MC, Ho CC, Kim JH (1998) Colloid Polym Sci 276:709
56. Tent A van (1992) PhD thesis. Delft University of Technology, Delft, The Netherlands, p 71